Int. J. Heat Mass Transfer. Vol. 28, No. 2, pp. 459–466, 1985
Printed in Great Britain

0017-9310/85 $3.00 + 0.00
Pergamon Press Ltd.

An experimental method to determine temperature-dependent extinction coefficients and solid thermal conductivities of glass fibre insulations in calorimetric measurements

H. REISS and B. ZIEGENBEIN
Brown, Boveri and Cie AG, Central Research Laboratory, Eppelheimer Strasse 82, D-6900 Heidelberg, F.R.G.

(*Received* 6 *February* 1984)

Abstract—This paper describes an experimental method to separate the two heat transfer mechanisms in evacuated fibre insulations. The method uses measured local thermal conductivities which are determined from the total heat flow through the insulation and the temperature profile. A regression analysis demonstrates a linear relationship with temperature of the solid conduction part of the total thermal conductivity and of the total extinction coefficient, to be a reasonable approximation.

INTRODUCTION

ONLY advanced high-temperature batteries provide sufficiently high energy and power densities for electric vehicle propulsion to be an economic alternative to gasoline powered cars. By means of thermal management the battery is maintained within a specified temperature range. The battery requires improved insulation to prevent excessive heat loss during long idle periods, a heating system to raise the battery cells to their operating temperature and a cooling system to prevent overheating during high-rate discharge (Fischer *et al.* [1]). Thermal model calculations for a 50-kWh passenger car battery lead to specific heat losses of less than 60 W m^{-2} at 320°C or effective thermal conductivities lower than 2.5×10^{-3} W m^{-1} K^{-1}. The need for a high-performance and lightweight vacuum insulation is obvious. A lightweight vacuum insulation requires a thin, leak-tight metal vacuum casing and an insulation material with very low degassing rates and withstanding atmospheric pressure load.

Recent experimental results of load-bearing vacuum insulation development indicate that, for powder insulations, the solid conduction seems to be too high to meet the above given design value (Reiss [2]) if the powder density cannot be reduced to about 0.2 g cm^{-3}. Nowobilski [3] measured thermal conductivities for the best continuous load-bearing fibre-board system of 3.2×10^{-3} W m^{-1} K^{-1} between 300 and 325°C. A quantitative knowledge of the relative amounts of combined radiative/solid conduction heat transfer rates in fibre-board insulations significantly facilitates further improvements of lower conductivity materials.

The present paper describes an experimental method to separate the two heat transfer mechanisms in evacuated fibre-board insulations leading to temperature-dependent extinction coefficients and solid conductivities. Adoption of this method to plain glass fibre insulations clearly shows that increasing the extinction, by using higher density boards, cannot sufficiently reduce radiative heat transfer for the above high temperature application.

EXPERIMENTAL PROCEDURE

Thermal conductivity measurement

Measurement of thermal conductivities is performed in a guarded hot plate calorimeter with two cold reference plates (Fig. 1). Testing was performed under varying residual gas pressure from less than 10^{-2} to 10^{5} N m^{-2}, compressive load from less than 0.01 to 0.3 M N m^{-2} and hot plate temperatures from 120 to 475°C (Ziegenbein [4]). The fact that the lateral heat flow in compressed multilayer insulation may be a factor 10^{2}–10^{3} greater than that perpendicular to the layer surface requires a uniform lateral temperature, i.e. very precise measurement of test section plate (11 cm diameter) and guard ring temperatures. An auxiliary heater attached to the outer guard ring minimizes additional heat losses through temperature sensor and resistance heater wires. The typical dimensions of insulation samples to be tested are $25 \times 25 \times 1$ cm. Depending on the type of insulation it generally took about 12 h to reach steady-state conditions.

Plain and opacified fibrous system insulations were made from binderless borosilicate glass fibre materials (0.69–1.1 μm diameter) (Johns Manville; 475-Tempstran; Code 108 A). For the Al_2O_3 insulation sample a 99% Al_2O_3 ceramic fibre (5 μm diameter) has been used (Didier GmbH, Wiesbaden, F.R.G.).

Figure 2 shows effective thermal conductivities for three different insulation samples. The temperature dependency for mean temperatures between 90 and 210°C could be fitted within the experimental error by a linear curve.

NOMENCLATURE

A	area of insulation sample [m^2]
$a_1, b_0, b_1, c_1, c_2, c_3$	constants
d	thickness of insulation layer [m]
d_0	total thickness of insulation [m]
$\bar{d}$	fibre diameter [μm]
E	total extinction coefficient [m^{-1}]
E_R	Rosseland mean of total extinction coefficient [m^{-1}]
$I_{\tilde{\lambda}b}$	hemispherical spectral emissive power of black body [W m^{-2} μm^{-1}]
m	porosity
n	real part of complex index of refraction
p	mechanical pressure on insulation sample [N m^{-2}]
$\dot{Q}$	total heat flow [W]
Q_{ext}	efficiency factor for total extinction
T	temperature [°C or K]
T_1, T_2	temperature of hot and cold sides of insulation, respectively [°C or K]
T_{x_i}	temperature of insulation sample at position x_i, $(0 \leqslant x_i \leqslant d_0)$ [°C or K]
T^{*3}, $T^{*3}_{1,2}$ or $T^{*3}_{x_i,i+1}$	radiation temperature calculated with T_1, T_2 or T_{x_i}, $T_{x_{i+1}}$ [K^3]
x_i	position within insulation [m]
Y	Young's modulus of elasticity [N m^{-2}].

Greek symbols

α	ratio of circumference of scattering particle to wavelength: $\alpha = \pi\bar{d}/\tilde{\lambda}$
κ	surface density of thin insulation layer [g cm^{-2}]
λ	total thermal conductivity [W m^{-1} K^{-1}]
λ_{eff}	effective total thermal conductivity measured over total insulation thickness [W m^{-1} K^{-1}]
λ_{SC}	solid conduction part of λ [W m^{-1} K^{-1}]
λ_T	thermal conductivity of solid material from which the fibres are made [W m^{-1} K^{-1}]
$\tilde{\lambda}$	wavelength [μm]
μ	Poisson number
ρ	density of fibre insulation [g cm^{-3}]
ρ_0	density of solid material from which the fibres are made [g cm^{-3}]
σ	Stefan–Boltzmann constant
τ_o	optical thickness.

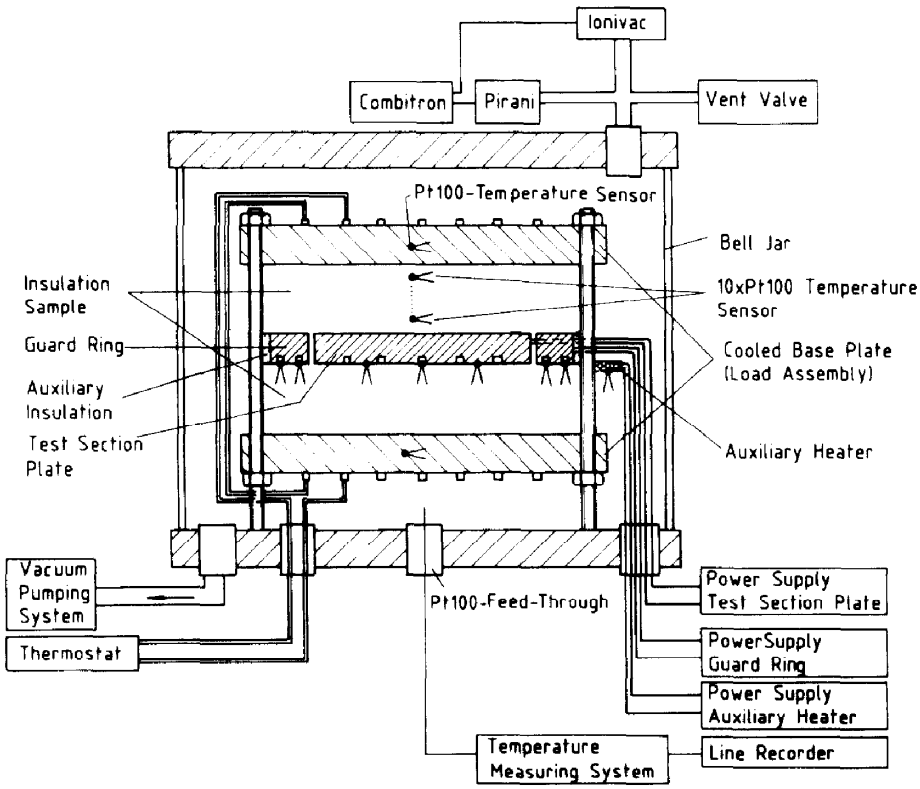

FIG. 1. Schematic diagram of a guarded hot plate calorimeter.

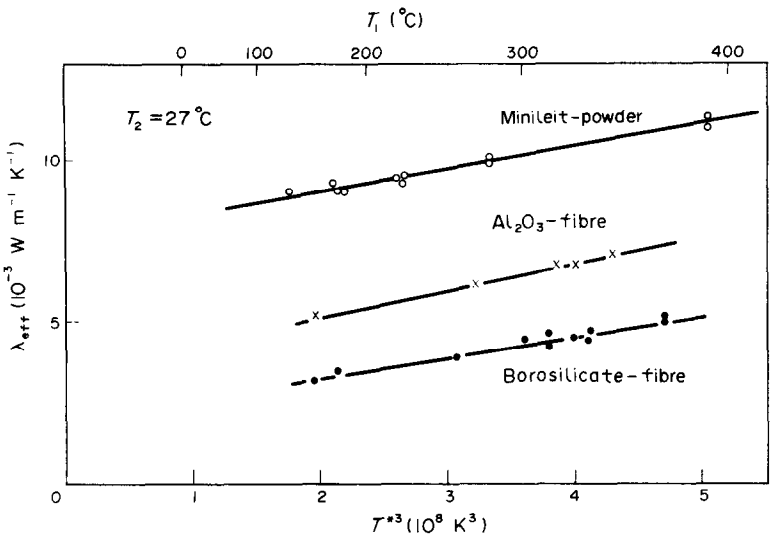

FIG. 2. Measured effective total thermal conductivities vs radiation temperature of evacuated powder and fibre insulations.

Temperature profile measurements

Reduction of solid conductivities and increase of extinction coefficients controlled by temperature profiles in the insulation, requires highly accurate temperature measurements. Up to 10 calibrated Pt 100 sensors were inserted at different positions in the upper insulation sample (Fig. 1). The exact position with respect to the distance from the cold plate of each sensor is given by the layer number. Uniform horizontal temperature distribution was controlled by inserting up to three sensors in the same layer. A disturbance of the temperature profile by the sensors could be neglected by increasing the sample thickness to 35 mm, and using 0.1 mm diameter wires for special small size Pt 100 sensors (Heraeus GmbH, Hanau, F.R.G., Type FKG 1030, 6).

The shapes of the measured temperature profiles in Fig. 3 clearly indicate the different solid conduction/radiation heat transfer ratios. For the low density insulation, high radiation transfer leads to a strongly curved temperature distribution, where approx. $\frac{4}{5}$ of the insulation thickness is required to decrease the local temperature to 50% of the hot side value. A nearly linear slope for the lowest curve results

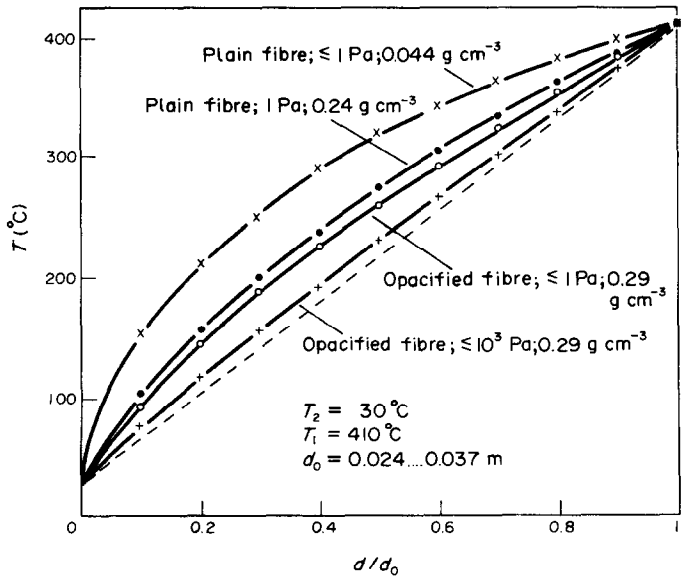

FIG. 3. Measured temperature profiles $T(x_i)$ in fibre insulations vs dimensionless position. The labels to the curves indicate: type of insulation, residual gas pressure and density, respectively.

from prevailing gas conduction (residual pressure 10^3 N m^{-2}) and high radiation extinction.

METHOD OF ANALYSIS

Based on the standard diffusion model, the following solution for the total thermal conductivity, λ, of a fibrous insulation operating in vacuum and bounded by opaque surfaces can be derived:

$$\lambda = \lambda_{sc} + 4/3\sigma n^2 T^{*3}_{1,2}/E \quad (1)$$

with $T^{*3}_{1,2} = (T_1^2 + T_2^2) \times (T_1 + T_2)$ where T_1 and T_2 are the hot and cold boundary temperatures, σ the Stefan–Boltzmann constant, n the real part of the effective index of refraction and E the extinction coefficient. For high optical thickness insulations studied here, the above additive approximation is valid. Thus from $(\lambda, T^{*3}_{1,2})$-plots in Fig. 2, λ_{sc} and E can be extracted from the intercept and slope for different insulation materials in the comparatively small temperature range 10^8 K$^3 \leqslant T^{*3}_{1,2} \leqslant 5 \times 10^8$ K^3.

In contrast to the above frequently used procedure, the method described here allows calculation of temperature-dependent solid conductivities and extinction coefficients by combining experimental calorimetric λ-data with measured temperature profiles in the insulation. For one set of boundary temperatures T_1 and T_2, the specific total heat flow in the insulation, $\dot{Q}/A$, is constant (A, area of test section plate). Local thermal conductivities $\lambda(x_i)$ are derived from

$$\lambda(x_i) = -\dot{Q}/A \times (x_i - x_{i+1})/(T_{x_i} - T_{x_{i+1}})$$

where T_{x_i} are the temperatures at the insulation layer positions x_i.

A plot of local conductivities, $\lambda(x_i)$, vs $T^{*3}_{x_i,i+1} = (T^2_{x_i} + T^2_{x_{i+1}}) \times (T_{x_i} + T_{x_{i+1}})$, in Fig. 4 shows for high density evacuated fibre insulations, there is no longer a linear relationship within the whole range of T^{*3}_x. This observation can be interpreted as λ_{sc} and E, in reality, not to be constant with respect to the temperature in the insulation. Furthermore, it should be noted that the T^{*3}_x-values in Fig. 4 extend to considerably higher values than $T^{*3}_{1,2} = (T_1^2 + T_2^2) \times (T_1 + T_2)$ in Fig. 2.

Temperature variation of extinction and solid conductivity

Assuming temperature-dependent $\lambda_{sc}(T)$ and $E(T)$, differentiation of equation (1) yields

$$\frac{d\lambda}{dT^{*3}} = \frac{d\lambda_{sc}(T)}{dT^{*3}} + \frac{4\sigma n^2}{3} \times \left[\frac{1}{E(T)} - \frac{T^{*3}}{E(T)^2} \times \frac{dE(T)}{dT^{*3}}\right]. \quad (2)$$

Obviously, λ should be linear in T^{*3} (index 1, 2 omitted) if both λ_{sc} and E are constant or linear in T^{*3}. A linearity of λ has been observed only in low-density fibre insulations (Fig. 4) with relatively small solid conductivities and extinction coefficients. For high-density or opacified samples, the nonlinearity of λ must be explained by a temperature dependency of E and/or λ_{sc}.

A possible temperature variation of E was investigated by calculating for a given temperature distribution, the Rosseland mean $E_R(T)$ (Siegel and Howell [5]), using measured spectral attenuation data of low optical thickness samples in the wavelength region $1 \leqslant \bar{\lambda} \leqslant 50$ μm. Except for the low temperature region, $E_R(T)$ in Fig. 5 can be quite well approximated by $E_R(T) = a_1 \times T$.

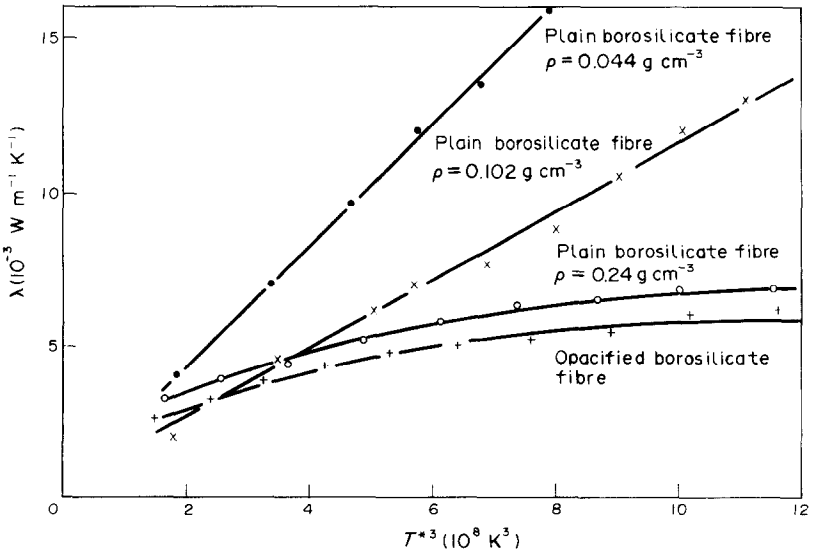

FIG. 4. Measured local total thermal conductivities vs radiation temperature.

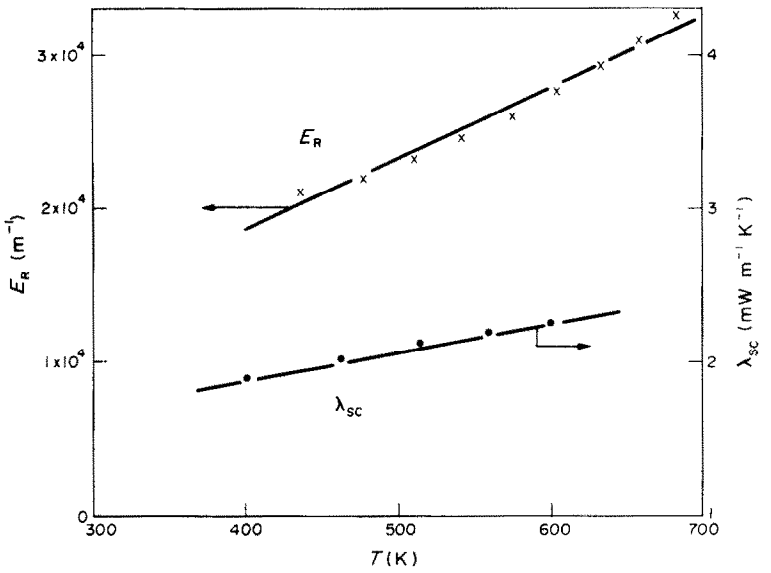

FIG. 5. Calculated Rosseland mean of total extinction coefficient, E_R, and solid conduction part, λ_{SC}, of total thermal conductivity of a borosilicate fibre board vs temperature.

A temperature dependency for λ_{sc} is derived in a formula given by Kaganer [6]:

$$\lambda_{sc}(T) = \frac{16(1-m)^2}{\pi^2} \times \frac{\lambda_T}{\frac{1}{1.86Ap^{1/3}} + \frac{1}{4(1-m)}}.$$

Here m denotes the porosity of the fibres, λ_T the thermal conductivity of the solid material the fibres are made from, and p the mechanical pressure on the sample. The factor A is used to calculate the contact radius between two fibres according to Hertz' formula,

$$A = \left(\frac{1-\mu^2}{Y(1-m)^2}\right)^{1/3},$$

where Y is the Young's modulus of elasticity and μ the Poisson coefficient. It is shown by Espe [7] that Y is proportional to the dynamic viscosity which in turn decreases exponentially with temperature. Therefore, it is not at all obvious that frequently made assumptions, like $\lambda_{sc}(T)$ = constant, are justifiable. Using Y-, μ- and λ_T-data for borosilicate glasses, the Kaganer formula yields an almost linear relationship of λ_{sc} and T in the interval $400 \leqslant T \leqslant 600$ K as shown in Fig. 5:

$$\lambda_{sc}(T) = b_0 + b_1 \times T.$$

where b_0, b_1 are constants. Inserting the approximations for $E_R(T)$ and $\lambda_{sc}(T)$ tentatively in equation (1),

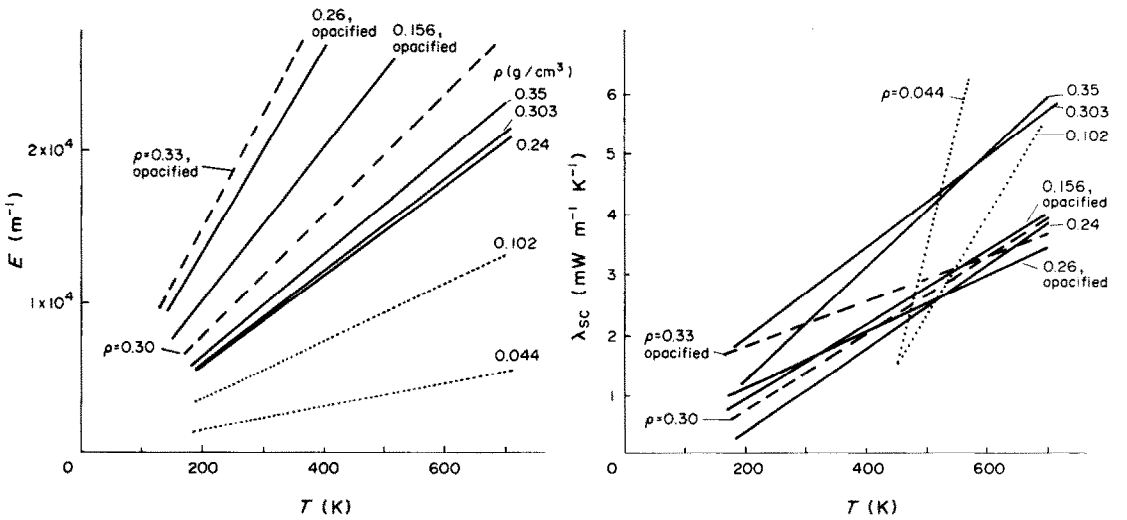

FIG. 6. Experimental total extinction coefficients, E, and solid thermal conductivities, λ_{SC}, of plain and opacified borosilicate fibre insulations vs temperature (solid and dashed lines, glass fibre papers; dotted lines, glass wool).

the thermal conductivity is given by:

$$\lambda = b_0 + b_1 T + \tfrac{16}{3} n^2 \sigma T^2 / a_1.$$

The radiation temperature T^* has been substituted by the local temperature $T = (T^{*3}/4)^{1/3}$ in the interval $T_{x_i} \leqslant T \leqslant T_{x_{i+1}}$. The temperature coefficient, a_1, of the extinction was calculated from the slope of the $(d\lambda/dT, T)$-plot. Subtraction of the radiative component from the measured total conductivity according to equation 3 gives the solid thermal conductivity $\lambda_{sc}(T)$. Figure 6 contains experimental extinction coefficients and solid conductivities for several plain and opacified fibre insulations. It should be noted that the nonlinear (λ, T^{*3})-curves in Fig. 2 are quite well explained by temperature-dependent extinction coefficients and solid conductivities, but that a linear relationship, as shown in Fig. 6, is only one possible assumption which might be justified by the theoretical consideration according to Fig. 5.

RESULTS

Measured temperature profiles of various plain and opacified borosilicate fibre insulations have been analysed by fitting their thermal conductivities by the following four assumptions for a possible temperature dependency:

$$\lambda = \lambda_{sc}(T) + \frac{4\sigma}{3} T^{*3}/E(T)$$

with

(a) $\lambda_{sc}(T) =$ constant and $E(T) =$ constant
(b) $\lambda_{sc}(T) = b_0 + b_1 T$ and $E(T) =$ constant
(c) $\lambda_{sc}(T) = b_0 + b_1 T$ and $E(T) = a_1 T$
(d) $\lambda_{sc}(T) = b_0 + b_1 T$ and $E(T) = a_1 T^2$.

Systematically, temperature dependencies of λ_{sc} and E according to (b) and (c) yielded far better fits to experimental data than (a) or (d). It must be concluded, that the solid conductivity of fibrous insulations has definitely to be taken increasing with temperature and that a temperature variation of the extinction coefficient seems to be probable because of the theoretical $E_R(T)$ in Fig. 5. Inserting into equation (2), we have $d\lambda/dT^{*3}\ c_1/x^{2/3}$ or $\lambda = c_2 x^{1/3} + c_3$, where $x = T^{*3}$ and c_1, c_2 and c_3 are constants. This result explains the (λ, T^{*3})-curves of the high density insulations in Fig. 4. A decision between (c) and (d) from calorimetric λ-data, however, can be made only after a further experiment when the total experimental error is reduced below 5%.

DISCUSSION

The measured calorimetric $E(T)$ in Fig. 6 can be attributed to absorption and/or scattering mechanisms. Pure or dominating scattering would lead to a more or less linear temperature profile if $\lambda_{sc}(T)$ = constant. Since Fig. 6 shows that $\lambda_{sc}(T)$ is definitely temperature dependent, calorimetric measurements cannot reveal whether scattering or absorption is dominating. However, evaluation of measured specific extinction coefficients $E/\rho = \tau_0/\kappa$ show scattering as the prevailing extinction mechanism at short wavelengths, i.e. in the high-temperature regions of the insulation samples ($\tau_0 = E \times d$, optical thickness; κ, specific surface density in g cm^{-2}).

Figure 7 shows a comparison of measured and calculated τ_0/κ-values for glass fibre samples with mean fibre diameter, $d = 1$ μm and solid glass density, $\rho_0 = 2.61$ g cm^{-3}. Micrographs of the fibre-board in Fig. 8 confirm that individual fibres in the compressed board

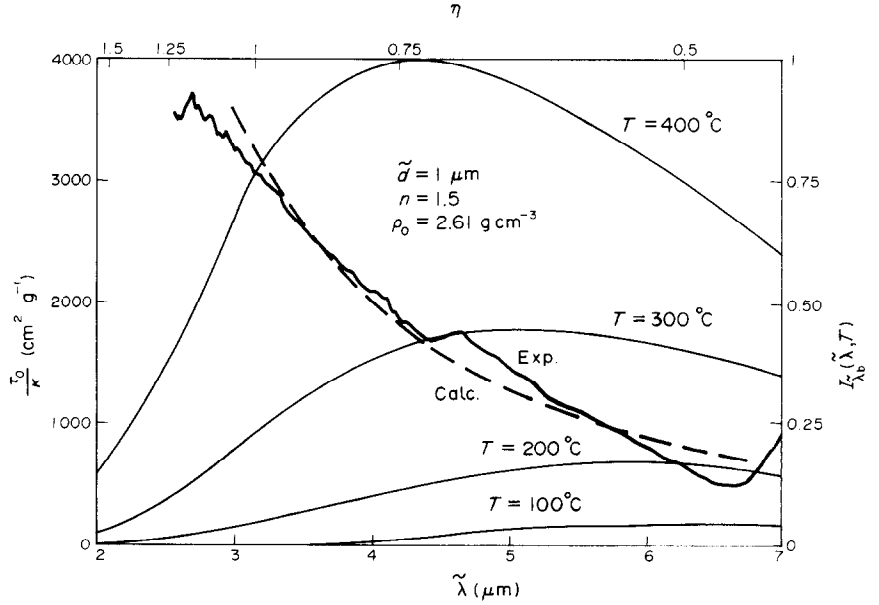

FIG. 7. Measured and calculated specific optical thickness, τ_0/κ, of a plain glass fibre insulation vs wavelength, $\tilde{\lambda}$. The black body hemispherical spectral emissive power, $I_{\tilde{\lambda}b}(\tilde{\lambda}, T)$, is given for orientation (normalized to unity).

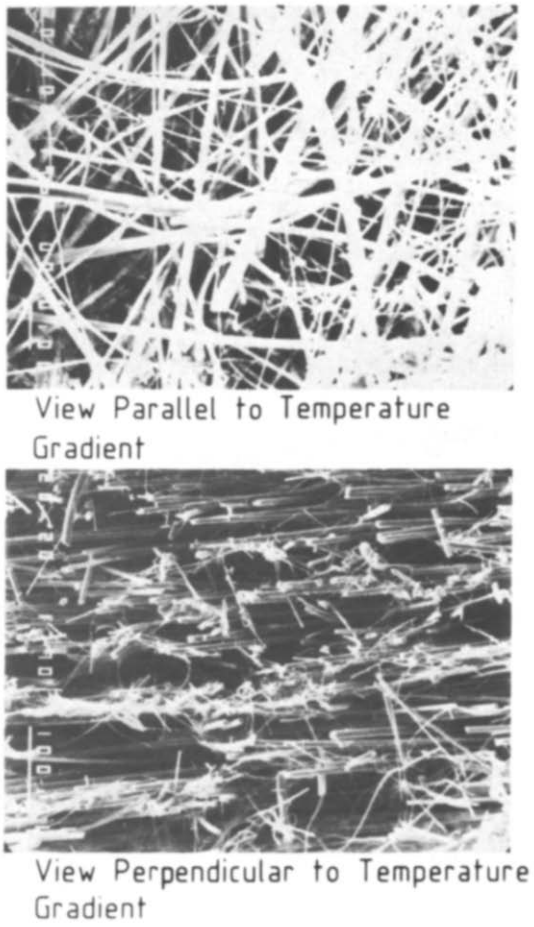

FIG. 8. Micrographs (scanning) of a plain borosilicate fibreboard.

are randomized in planes perpendicular to heat flow. Measured τ_0/κ are taken from Caps *et al.* [8]. Theoretical values have been calculated using a constant index of refraction $n = 1.5$, and an appropriate expression for the extinction cross-section for perpendicular incidence of unpolarized radiation on very long cylinders. Van de Hulst [9] has shown that the efficiency factor for extinction, Q_{ext}, for a real refractive index near to 1 approaches for small η the value $Q_{ext}(\eta) = \frac{2}{3}\eta^2$ for both orientations of the electric vector with respect to the fibre axis, where η is given by $\eta = 2(n-1)\alpha$ and $\alpha = \pi \times \tilde{d}/\tilde{\lambda}$.

This expression for $Q_{ext}(\eta)$ and the following equation for the specific extinction coefficient $E/\rho = 4/\rho_0 \times Q_{ext}/(\alpha \times \tilde{\lambda})$ yield the theoretical (dashed) curve in Fig. 7. Multiple scattering is considered to be negligible in the transmission measurement since the optical thickness of this sample was very low. No account has been made for the distribution of the real fibres with respect to their diameter and orientation to the incident beam. The relatively good approximation of measured by calculated extinctions leads to the conclusion that at least for $T \geqslant 200°C$ (anisotropic) scattering is the predominant extinction mechanism. This is in accordance with measurements of the spectral albedo for fibre insulations from Cabannes *et al.* [10] and extended calculations of Caps *et al.* [8].

REFERENCES

1. W. Fischer, F. Gross, D. Hasenauer, H. Kahlen and K. Liemert, A passenger car..., in *Proc. 30th Int. Power Sources Symp.*, Atlantic City, 1983. The Electrochem. Soc., Princeton, New Jersey, p. 59 (1983).
2. H. Reiss, Evacuated, load bearing powder insulation for high temperature applications, *J. Energy* **7**, 152 (1983).
3. J. J. Nowobilski, Insulation development for high-temperature batteries for electric vehicle application, Final Report, Union Carbide, Linde Division, Tonawanda, New York, Contract No. EM-78-C-01-5160 (1979).
4. B. Ziegenbein, Evacuated high temperature insulations for electrochemical batteries, in Proceedings of the 8th Europ. Conf. Thermosphys. Prop., Baden-Baden F.R.G., 1982. *High Temp.–High Press* **15**, 329 (1983).
5. R. Siegel and J. R. Howell, *Thermal Radiation Heat Transfer*. p. 487, McGraw-Hill, Kogakusha, Tokyo (1972).
6. M. G. Kaganer, Thermal insulation in cryogenic engineering, Trans. from Russian by A. Moscona. *Israel Progr. Sci. Trans., Jerusalem* (1969).
7. W. Espe, *Werkstoffkunde der Hochvakuumtechnik*, Vol. II. VEB Deutscher Verlag der Wissenschaften, Berlin (1960).
8. R. Caps, A. Trunzer, D. Büttner, J. Fricke and H. Reiss, Spectral transmission and reflexion properties of high temperature insulation materials and their relation to radiative heat flow. *Proc. 18th Int. Thermal Cond. Conf., Rapid City, 1983*, in print.
9. H. C. Van de Hulst, *Light Scattering by Small Particles*, p. 297. Dover, New York (1981).
10. F. Cabannes, J.-C. Maurau, M. Hyrien and S. M. Klarsfeld, Radiative heat transfer in fibreglass insulating materials as related to their optical properties. *High Temp.–High Press* **11**, 429 (1979).

UNE METHODE EXPERIMENTALE POUR DETERMINER LES COEFFICIENTS D'EXTINCTION ET LES CONDUCTIVITIES THERMIQUES DES ISOLANTS EN FIBRES DE VERRE, PAR DES MESURES CALORIMETRIQUES

Résumé—On décrit une méthode expérimentale pour séparer les deux mécanismes de transfert thermique dans les isolants fibreux. La méthode utilise les conductivités thermiques locales mesurées qui sont déterminées à partir du flux thermique total et du profil de température. Une analyse de régression montre qu'une relation linéaire avec la température de la conductivité du solide et du coefficient total d'extinction est une approximation raisonnable.

EIN EXPERIMENTELLES VERFAHREN ZUR BESTIMMUNG DER TEMPERATURABHÄNGIGEN EXTINKTIONSKOEFFIZIENTEN UND WÄRMELEITFÄHIGKEITEN VON GLASFIBER-ISOLIERMATERIALIEN DURCH KALORIMETRISCHE MESSUNGEN

Zusammenfassung—Diese Arbeit beschreibt ein experimentelles Verfahren, um die beiden Wärmetransport-Mechanismen, die in evakuierten Glasfiber-Isoliermaterialien auftreten, zu trennen. Das Verfahren verwendet Meßwerte der örtlichen Wärmeleitfähigkeit, welche aus dem Gesamt-Wärmestrom und dem Temperaturprofil ermittelt worden sind. Mit Hilfe der Regressionsanalyse wird gezeigt, daß die lineare Abhängigkeit des Festkörperanteils der Gesamt-Wärmeleitfähigkeit und des Gesamt-Extinktionskoeffizienten von der Temperatur eine annehmbare Näherung darstellt.

ЭКСПЕРИМЕНТАЛЬНЫЙ МЕТОД ОПРЕДЕЛЕНИЯ ЗАВИСЯЩИХ ОТ ТЕМПЕРАТУРЫ КОЭФФИЦИЕНТОВ ЗАТУХАНИЯ И ТЕПЛОПРОВОДНОСТИ ТВЕРДОЙ ФАЗЫ СТЕКЛОВОЛОКНИСТЫХ ИЗОЛЯЦИОННЫХ МАТЕРИАЛОВ ПРИ КАЛОРИМЕТРИЧЕСКИХ ИЗМЕРЕНИЯХ

Аннотация—Описывается экспериментальный метод, позволяющий разграничить два механизма теплопереноса в вакуумированных волокнистых изоляционных материалах. Метод основан на определении локальных значений теплопроводности по суммарному потоку тепла через изоляционный материал и по температурному профилю. С помощью регрессионного анализа показано, что хорощей аппроксимацией является линейная зависимость от температуры суммарного коэффициента затухания и той части полного коэффициента теплопроводности, которая связана с переносом через твердые волокна изоляции.